Qatar Univ. Sci. J. (1992), 12: 8 -13

A NUMERICAL SOLUTION FOR THE BENDING OF A PLATE USING THE BOUNDARY ELEMENT METHOD

By

MEDHAT M. ABBASSI
Mathematical Department, Alexandria University, Egypt

الحـــل العـــددي لصفيحـــة ملتويـــة باستخــــدام طريقـــة العنصـــر الحـــدي

مـدحـــت عبـــاسي

لقد تم في هذا البحث إعتبار الحل العددي لصفيحة ملتوية . والطريقة المستخدمة تسمى طريقة العنصر الحدي .

وهذه الطريقة تعتمـــد أساساً على تكوين المعادلة التكاملية الحدية لمعادلة تفاضلية جزئيـة باستخدام حلها الأســاسي .

ABSTRACT

In this paper the numercial solution for the bending of a plate is considered. The method used is called the Boundary Element Method (BEM). The BEM is a numerical method based on the boundary integral equation formulation of a partial differential equation using its fundamental solution.

Key Words: Numerical solution, Bending of a plate, Boundary element method.

I. A Boundary Integral equation Formulation for a plate Equation with Prescribed Boundary Displacement and Rotation Data.

In this paper the numerical solution for the bending of a plate is considered. The plate is modelled by a biharmonic equation with no loading and with boundary displacement and rotation data given, as shown below.

$$\Delta^2\psi(X) = 0 \qquad X \in \Omega$$

$$\psi(X) = f_1(X) \qquad X \in \partial\Omega \qquad (1.1)$$

$$\frac{\partial}{\partial n} = f_2(X) \qquad X \in \partial\Omega$$

where $\Delta = \sum_{1=1}^{2} \frac{\partial^2}{\partial X_i^2}$ $X = (X_1, X_2) \in \Omega \subset R^2$

$\partial\Omega$ = boundary of Ω

n = Unit outward normal on $\partial\Omega$

The method used is called the Boundary Element Method (BEM). The BEM is a numerical method based on the boundary integral equation formulation of a partial differential equation using its fundamental solution. This method has gained rapid popularity in recent years. Let us sketch its usage here for our problem.

Let G(x, X) denote the fundamental solution of the biharmonic equation satisfying

$$\Delta^2 G(x, X) = \delta(x, X) \qquad x, X \in IR^2 \qquad (I.2)$$

where δ is the Dirac delta distribution.

Set

$$F(x, X) = \Delta G(x, X)$$

Then (I.2) becomes

$$\Delta F(x, X) = \delta(x, X)$$

Thus F(x, X) is the fundamental solution of the harmonic equation

$$\Delta\psi(X) = 0$$

So we get

$$F(x, X) = \frac{1}{2\pi} \ln|x-X|$$

or

$$\Delta G(x, X) = \frac{1}{2\pi} \ln|x-X| \qquad (I.3)$$

Assume that X = 0, r = |x|. Then (1.3) can be written as

$$\frac{1}{r}\frac{\partial}{\partial r}\left(r\frac{\partial G}{\partial r}\right) = \frac{1}{2\pi}\ln r$$

Solving the above differential equation we obtain

$$G(x, X) = \frac{1}{8\pi}(r^2 \ln r) = \frac{1}{8\pi}|x-X|^2 \ln|x-X| \qquad (I.4)$$

Our work here is based on the following integral representation of the solution ψ:

$$\psi(X) = \int_{\partial\Omega} [\alpha(x)\, G(x, X) + \beta(x)\, B_{2X}\, G(x, X)]\, d\sigma_X \quad (I.5)$$

($d\sigma_X$ = infinitesmial boundary measure with respect to the variable x), where B_{2X} is a boundary integral operator corresponding to the bending moment of the plate defined by

$$B_2 = \upsilon\Delta + (1-\upsilon)\left[n_1^2 \frac{\partial^2}{\partial x_1^2} + n_2^2 \frac{\partial^2}{\partial x_2^2} + 2n_1 n_2 \frac{\partial^2}{\partial x_1\, \partial x_2}\right] \qquad (I.6)$$

υ = The poisson ratio.

In (I.5), $\alpha(x)$ and $\beta(x)$ are unknown displacement and moment density functions on $\partial\Omega$ to be determined. (I.5) is called the integral equation formulation for (I.1). A regorous justification of (I.5) is rather lengthy and will appear elsewhere.

The representation (I.5) is valid for $X \epsilon\, \partial\Omega$. Now let $X \rightarrow \overline{X} \epsilon\, \partial\Omega$. As the kernels $G(x, X)$ and $B_2X\, G(x, X)$ are absolutely integrable functions with respect to x even for $X \epsilon\, \partial\Omega$, we obtain

$$\psi(X) = \int_{\partial\Omega} [\alpha(x)\, G(x, \overline{X}) + \beta(x)\, B_{2x}\, E(x, \overline{X})]\, d\sigma_X \text{ for } X \epsilon\, \partial\Omega. \quad (I.7)$$

If $\beta \,\epsilon\, L^2(\partial\Omega)$. Nevertheless, the above continuity property does not carry over to the normal derivative $\frac{\partial\psi}{\partial n}$ (i.e., rotation). In fact, from a boundary layer property of singular integrals, we have

$$\frac{\partial\psi(\overline{X})}{\partial n} = \int_{\partial n}\left[\alpha(x)\frac{\partial}{\partial n_X} E(x, \overline{X}) + \beta(x)\frac{\partial}{\partial n_X} B_{2X}G(x, \overline{X})\right] d\sigma_X - \frac{1}{2}\beta(X) \qquad (I.8)$$

provided that $\partial\Omega$ is smooth at $\overline{X}$. If $\partial\Omega$ is not smooth at $\overline{X}$ then a different weighting factor (other than ½) of $\beta(\overline{X})$ on the right hand side of (I.8) must be properly adjusted according to the angle θ formed by the tangents to $\partial\Omega$ at $\overline{X}$.

On the right hand side of (I.8), as the kernel $\frac{\partial}{\partial n_X} B_{2X}\, G(x, X)$ now contains a singularity when $x - X$, the boundary integral must be interpreted as Cauchy principal value (singular integral):

$$\int_{\partial\Omega} \beta(x)\frac{\partial}{\partial n_X} B_{2X}G(x, \overline{X})\, d\sigma_X = \lim_{S\rightarrow 0} \int_{\partial\Omega - B_2} \beta(x)\frac{\partial}{\partial n_X} B_{2X}G(x, \overline{X})\, d\sigma_X$$

where, B_e is an e-ball centered at $\overline{X}$:

$$B_e = \{\, y \,\epsilon\, IR^2 \mid |\, y - \overline{X} > e \,\}$$

Substituting the boundary conditions in (I.1) into (I.7) and (I.8), we get

$$\int_{\partial\Omega} [\alpha(X)G(x, \overline{X}) + \beta(X)\, B_{2X}G(x, \overline{X})]\, d\sigma_X = f_1(\overline{X}), \overline{X} \epsilon\, \partial\Omega \quad (I.9)$$

$$\int_{\partial\Omega}\left[\alpha(x)\frac{\partial}{\partial n_X} G(x, \overline{X}) + \beta(x)\frac{\partial}{\partial n_X} B_{2X}G(x, \overline{X})\right] d\sigma_X - \frac{1}{2}\beta(\overline{X}) = f_2(\overline{X}),\ \overline{X} \epsilon\, \partial\Omega$$

where the right hand sides are known. The above becomes a system of Fredholm boundary integral equations of mixed first and second kinds for the displacement density data $\alpha(x)$ and bending moment density data $\beta(x)$ on $\partial\Omega$. If $\alpha(x)$ and $\beta(x)$ are solved everywhere on $\partial\Omega$, then we can use (I.5) to obtain the values of $\psi(X)$ for any $X \,\epsilon\, \Omega$.

II. The Numercial Alogarithm

One can solve (I.9) and (I.10) for $\alpha(x)$ and $\beta(x)$, for example; by dividing the boundary $\partial\Omega$ into n arcs, $A_1, A_2, \ldots A_n$. Each arc A_i is further approximated by a line segment L_i, as shown in Figure 1.

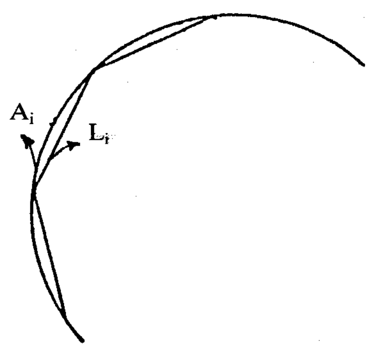

Figure 1

Then one assumes that $\alpha(x)$ and $\beta(x)$ are piecewise constant on the line segments. (I.9) and (I.10) becomes a system of 2n linear equations. TThis system can be solved by standad Gaussian elimination procedures for $\alpha(x)$ and $\beta(x)$. As $\alpha(x)$ and $\beta(x)$ are solved, one can use (I.5) to approximate $\psi(X)$ for $X \,\epsilon\, \Omega$.

In this paper, the problem is considered for a special case where Ω is a disk with radius R = 0.5. We take advantage of the geometry of the domain Ω where a polar coordinate system (r, θ) can be setup. We divide the boundary $\partial\Omega$ into n arcs, $A_1, A_2, \ldots$ A_n, using the angular variable θ. The arc A_i is represented by the subinterval $\left[\frac{2\pi}{n}(i-1), \frac{2\pi i}{n}\right]$

The smoothness of the boundary has been preserved, so higher order or spline approximations of $\alpha(\theta)$ and $\beta(\theta)$ are made possible.

Numerically we solve (I.9) and (I.10) for $\alpha(X)$ and $\beta(X)$ on $\partial\Omega$ as follows.

Let $x = re^{i\theta}$, $X = pe^{i\theta}$, so (1.9) and (I.10) can be written as

$$\int_0^{2x} [\alpha(\theta)\, G(\theta,\phi) + \beta(\phi)B_{2X}G(\theta,\phi)]\, R\partial\theta = f_1(\phi) \qquad (II.1)$$

$$\int_0^{2X}\left[\alpha(\theta)\frac{\partial}{\partial\rho}G(\theta,\phi) + \beta(\theta) - B_{2X}G(\theta,\phi)\right] R d\theta - \frac{1}{2}\beta(\phi) = f_2(\phi) \qquad (II.2)$$

we divide the boundary into n arcs $A_1, A_2, \ldots\ldots, A_n$, as shown below in Figure 2.

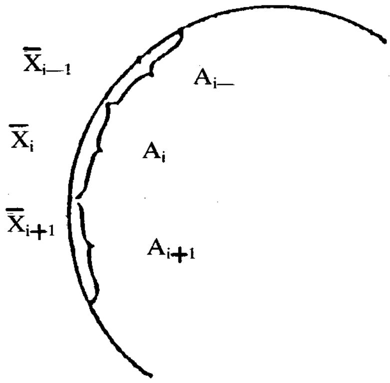

Figure 2

Denote the mid-point of each arc A_i by $\overline{X}_i$. Each point $\overline{X}_i$ is called a node.

We approximate $\alpha(X)$ and $\beta(X)$ on $\partial\Omega$ by piecewise constant functions i.e. piecewise constant boundary elements. On each A_j, $1 \leqslant j \leqslant n$, we assume that $\alpha(\theta)$ and $\beta(\theta)$ are constants.

$$\left.\begin{aligned} \alpha(\theta) &= \alpha(\overline{X}_j) \\ \beta(\theta) &= \beta(\overline{X}_j) \end{aligned}\right\} \text{for } \theta \in \left[\frac{2\pi}{n}(j-1), \frac{2\pi j}{n} \right]$$

where

$$\overline{X}_j = R\ e^{i\omega j} = R\ e^{\frac{\pi}{n}(2j-i)},\ j = 1, 2, \ldots, n$$

(If necessary, higher order or spline approximations can be used for $\alpha(\theta)$ and $\beta(\theta)$).

Consequently, (II.1) and II.2) can be discretized as

$$\sum_{j=1}^{n} \alpha(\theta_j) \int_{A_j} G(\theta,\phi_i)\, R\, d\theta + \sum_{j-1}^{n} \beta(\theta_i) \int_{A_j} B_{2X}G(\theta,\phi_i)\, R\, d\theta = f_1(\phi_i) \tag{II.3}$$

$$\sum_{j=1}^{n} \alpha(\theta_j) \int_{A_j} \frac{\partial}{\partial\rho} G(\theta,\phi_i)\ R\ d\theta + \sum_{j-1}^{n} \beta(\theta_j) \int_{A_j} \frac{\partial}{\partial\rho} B_{2x}G(\theta,\phi_i)\ R\ d\theta$$

$$-\frac{1}{2}\beta(\phi_i) = f_2(\phi_i) \tag{II.4}$$

for $i = 1, 2, \ldots, n$

Set

$$A_{ij} = \int_{A_j} B_{2X}\ G\ (\theta,\phi_i)\ Rd\theta$$

$$A_{i,n+j} = \int_{A_j} B_{2X}\ G\ (\theta,\phi_i)\ Rd\ \theta$$

$$A_{n+i,j} = \int_{A_j} \frac{\partial}{\partial\rho} G(\theta,\phi_i)\ R\ d\theta$$

$$A_{n+i,n+j} = \int \frac{\partial}{\partial\rho} b_{2X}\ G(\theta,\phi_i)\ R\ d\theta - \left| \begin{cases} 0 \text{ if } i=j \\ \frac{1}{2} \text{ if } i=j \end{cases}\right.$$

$$z_1 = \alpha\ (\theta_1)$$

$$Z_{n-i} = \beta(\theta_i)$$

$$D_i = f_i\ (\phi_i)$$

$$D_{n-i} = f_2\ (\phi_i)$$

then (II.3) and (II.4) can be written as a matrix equation

$$\begin{bmatrix} A_{11} & A_{12} \ldots A_{12n} \\ A_{21} & A_{22} \ldots A_{22n} \\ & \\ A_{2ni} & A_{2n2} \ldots A_{2n,2n} \end{bmatrix} \begin{bmatrix} Z_1 \\ Z_2 \\ \\ Z_{2n} \end{bmatrix} = \begin{bmatrix} D_1 \\ D_2 \\ \\ D_{1n} \end{bmatrix} \tag{II.5}$$

Or, briefly

$$AZ = D$$

The above is a system of 2n linear equations. It can be solved by standard Gaussian elimination procedures if all elements A_{jj}, $1 \leqslant i, j \leqslant 2n$ are obtained.

The method for obtaining A_{ij} ; is as follows

Setting $x = re^{i\theta}$, $X = \rho e^{i\theta}$, we have

$$G(x,X) = \frac{1}{10\pi}[r^2+\rho^2-2r\rho \cos(\theta-\phi)] \ln [r^2+\rho^2-2r\rho \cos(\theta-\phi)], \tag{II.6}$$

$$B_{2X}G(x,X) = \upsilon\triangle G + (1-\upsilon)\frac{\partial^2 G}{\partial r^2}$$

$$= \frac{1}{8\pi}\left\{ (1+\upsilon) \ln [\ r + 1\rho^2 - 2r\rho \cos(\theta-\phi)] + 4\rho \right| \tag{II.7}$$

$$+ (1-\upsilon)\left[1 + \frac{2[\rho - r\cos(\theta-\phi)]^2}{r^2\rho^2 - 2r\rho\cos(\theta-\phi)} \right] \Bigg\}$$

On $\partial\Omega$, $\rho=r=R$, we have

$$G(\theta,\phi) = \frac{R^2}{8\pi}[1-\cos(\theta-\phi)] \ln [2R^2\{1-\cos(\theta-\phi)\}] \tag{II.8}$$

$$\frac{\partial G(\theta-\phi)}{\partial n_X} = \frac{R}{8\pi}\Big\{[1-\cos(\theta-\phi)]$$

$$[\ln\{2R^2[1-\cos(\theta-\phi)]\} + 1]\Big\} \tag{II.9}$$

$$B_{2X}G(\theta-\phi) = \frac{1}{8\pi}\Big|\Big\{(1+\rho) \ln [2R^2\{1-\cos(\theta-\phi)\}] + 4\rho$$

$$+(1-\rho)[2-\cos(\theta-\phi)] \tag{II.10}$$

$$\frac{\partial}{\partial n_X} B_{2X}G(\theta,\phi) = \frac{1}{8\pi}[2\upsilon - (1-\upsilon)\cos(\theta-\phi)] \tag{II.11}$$

In the above we can see that except for $B_{2X}(\theta,\phi)$, all kernels

$G(\theta,\phi)$, $G(\theta,\phi)$ and $B_{2X}G(\theta,\phi)$ do not contain any singularity. So we can estimate terms A_{jj}, $A_{n-j,j}$ and $A_{n-j,n-j}$ by a Gaussian quadrature

$$\int_A^B g(x)\,dx = \frac{B-1}{2}\sum_{j=1}^{m} w(1)\, g\left[\frac{(B-A)\,S(1)+B+A}{2}\right]$$

where w(1)'s and S(1)s are, respectively, the coefficients and the roots in the Gaussian quadrature.

For

$$A_{i,n-j} = \int_{Aj} B_{2x}g(\theta,\phi_i)\ R\ d\theta,$$

when $i\neq j$, $B_{2X}G(\theta,\phi_i)$ does not contain any singularity for $\theta \in A_j$, so we can approximate A_i,n—j again by using a Gaussian quadrature, when $i = j$, $B_{2X}G(\theta,\phi_i)$ contains a singularity at $\theta = \phi I$. We treat it as follows:

Rewrite

$$\ln\{2R^2[1-\cos(\theta-\phi_i)]\}$$

$$= \ln 2R^2+\ln[1-\cos(\theta-\phi_i)]$$

$$= \ln 2R^2 - \ln[1+\cos(\theta-\phi_i)] + 2\ln[\sin(\theta-\phi_i)]$$

It follows that

$$A_{i,n+i} = \int_{Ai} B_{2X}G(\theta,\phi_i)\ Rd\theta$$

$$= \frac{R}{8\pi}\int_{\frac{2x}{n}(i-1)}^{\frac{2x}{n}i}\Big\{(1+\upsilon)[\ln 2R^2-\ln[1+\cos(\theta-\phi)]]+4\upsilon + (1-\upsilon)\,[-\cos(\theta-\phi_i)]\Big\}d\theta$$

$$+\frac{2R(1+\upsilon)}{(2\pi)}\int_{\frac{2x}{n}(i-1)}^{\frac{2x}{n}i}\ln[\sin(\theta-\phi_i)]\,d\theta$$

In the above, the first integrand is smooth so we use a Gaussian quadrature to approximate the integral. For the second integral, the integrand has a singularity at $\theta=\phi_i$. We can approximate it to as high degree of accuracy as desirable by

$$\int_0^{\alpha} \ln[\sin X]\,dx = \alpha\ln\alpha-\alpha-\frac{\alpha^3}{18}-\frac{\alpha^5}{900}-\frac{\alpha^7}{19045}-\cdots$$

Hence all entries $A_{j,j}$ of the matrix, A can be obtained. We then solve (II.3) and (II.4) for $\alpha(\theta)$ and $\beta(\theta)$ on $\partial\Omega$, and use (I.5) to solve all $\psi(X)$ for $X \in \Omega$. In (I.5), G(x,X) and B_{2X} G(x,X) are given by (II.6) and 11.7) rather than (II.8) and (II.10).

III. Numerical Examples

In our first numerical example we use the fundamental solution of the biharmonic equation to construct a solution, and use it as a benchmark to test our algorithm and to check the accuracy.

Example 1:

Let

$$\psi(X) = \frac{1}{8\pi}\{100|X-X_1|^2\ln|X-X_1|+40|X-X_2|^2\ln|X-X|$$
$$+30|X-X_3|^2\ln|X-X_3|+20|X-X_4|^2\ln|X-X_4|\}$$

where

$X_1 = (-1.5,\ 1.5)$, $X_2 = (2.0,\ 2.0)$,

$X_3 = (3.0,\ -3.0)$, $X_4 = (-2.5,\ -2.5)$

which all lie on the outside of Ω, so $\psi(X)$ is a solution of the biharmonic equation. Therefore we can use $\psi(X)$ together with ψ and $\frac{\partial\psi}{\partial n}$ on $\partial\Omega$ to test our algorithm. Table 1 shows the accuracy of our algorithm.

Table 1
[$N=10,\ X_i=(\frac{1}{3},\theta_i)$]

I	θ_i	Numerical solutions (υ=0.01)	Numerical solutions (υ=0.06)	Exact sol.
1	0.0000	71.6540	73.3192	71.4053
2	0.5236	70.9516	72.6101	70.7080
3	1.0472	70.6752	72.3307	70.4318
4	1.5708	70.9193	72.5770	70.6739
5	2.0944	71.5304	73.1943	71.2830
6	2.6180	72.2201	73.8906	71.9695
7	3.1416	72.7990	74.4749	72.5443
8	3.6652	73.2363	74.9163	72.9798
9	4.1888	73.5136	75.1966	73.2561
10	4.7124	73.5335	75.2169	73.2758
11	5.2360	73.1931	74.8730	72.9359
12	5.7596	72.5037	74.1770	72.2495

From the above, we can see that using smaller υ (the Poisson ratio) will yield a higher accuracy in the example. When $X\epsilon\Omega$ but very close to $\partial\Omega$, especially when X is very close to one of the end points of those arcs partitioned on $\partial\Omega$, the error in the computation of $\psi(X)$ becomes comparatively larger. As we observe in (II.7) we believe that this is due to the log term and the last term in (II.7). This is related to the boundary layer effect. To overcome this difficulty we use a quadratic interpolation. Note that $\psi(X)$, $x \in \partial\Omega$, is given when X is very close to $\partial\Omega$, $\psi(X)$ is also very close to $\psi(X)$ from some $x \in \partial\Omega$. Let $X \in \Omega$ be the point very close to $\partial\Omega$, at which we try to evaluate $\psi(X)$. Let Arg(X) be the argument of X. Then the point $X_0 = (R, \text{Arg}(X))$ is on the boundary and

$$|X-X_O| = \text{distance}\ (X,\ \partial\Omega)$$

As $\psi(X)$, $x \in \partial\Omega$, is given, we know $\psi(X_O)$ exactly. Then for $X_1 = (R-\triangle R, \text{Arg}(X))$ and $X_2 = (R-2\triangle R, \text{Arg}(X))$, we compute

$\psi(X_1)$ and $\psi(X_2)$ through (I.5) since X_1 and X_2 are not close to $\partial\Omega$. $\psi(X_1)$ and $\psi(X_2)$ are comparatively accurate. In our numerical examples, we take $\triangle R = 0.01$. Now we can see that all these four points X_0, X, X_1 and X_2 have the same argument Arg(X), so they are on the same ray. Along this ray, through $(X_0,\psi(X_0))$, $(X_1,\psi(X_1))$ and $(X_2,\psi(X_2))$, we use quadratic interpolation:

$$\psi(X)\approx\psi(X_0)\,\frac{(X-X_1)\ (X-X_2)}{(X_0-X_1)\ (X_0-X_2)} + \psi(X_1)\,\frac{(X-X_0)\ (X-X_2)}{(X_1-X_0)\ (X_1-X_2)}$$

$$+\psi(X_2)\,\frac{(X-X_0\ (X-X_1)}{(X_2-X_0)\ (X_2-X_1)}$$

to approximate $\psi(X)$. Table 2, Fig. 3 and Fig. 4 illustrate the improvement by interpolation.

Table 2

$N = 10,\ X_1 = (0.499,\theta_i),\ \upsilon = 0.01$

I	θ_i	Numerical solution	Solution thru interpolation	Exact solution
1	0.000	73.1948	73.2178	73.2176
2	9.5236	70.2769	72.1016	72.0167
3	1.0472	69.3203	71.6355	71.5960
4	1.5708	69.3975	72.0201	72.0198
5	2.0944	70.7693	73.0889	73.0496
6	2.6180	72.2664	74.1288	74.0884
7	3.1416	74.8129	74.8417	74.8416
8	3.6652	73.5625	75.4677	75.4216
9	4.1888	73.5453	75.9338	75.8933
10	4.7124	73.2659	76.0394	76.0394
11	5.2360	73.2659	75.6569	75.6162
12	5.7596	72.7042	74.6170	74.5774

SOLUTION ERROR COMPARISION

FIG·3

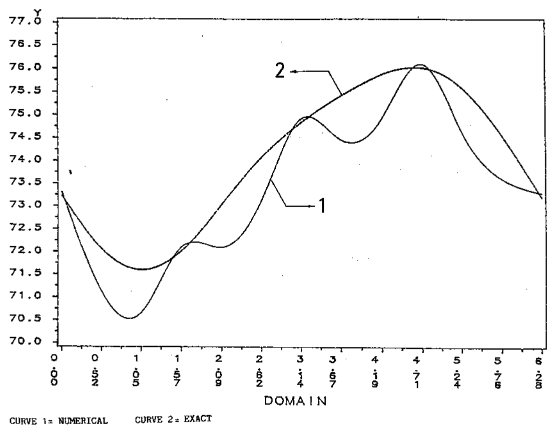

SOLUTION ERROR COMPARISION

FIG·4

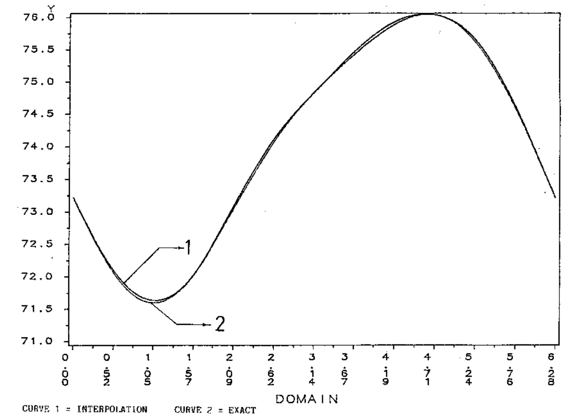

Fig. 5 is the graph of the exact solution and Fig. 6 is that of the numerical solution. By comparing then we have a visual display of the accuracy of our algorithm.

FIG·5 THE NUMERICAL SOLUTION

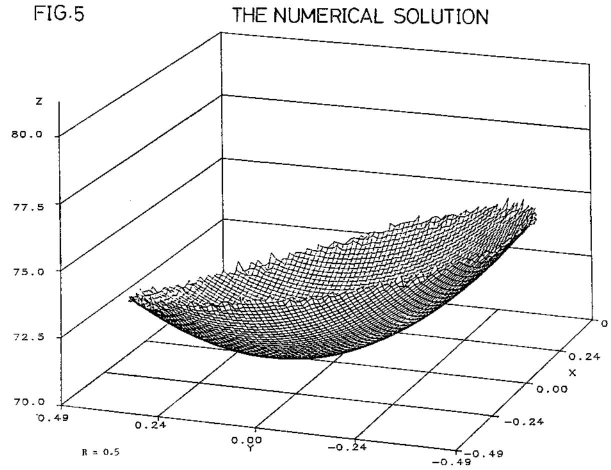

FIG·6 THE EXACT SOLUTION

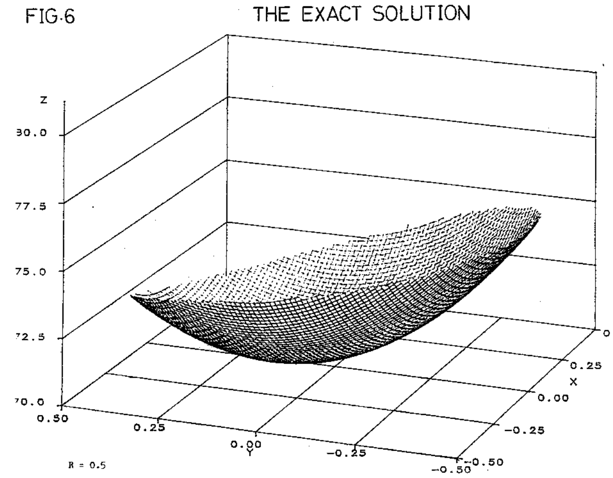

Example 2:

As the second numercial example, we solve the following bihormonic equation

$$\Delta^2\psi(X) = 0 \qquad X \in \Omega,$$
$$\psi(X) = 10\sin 2\theta \qquad X \in \partial\Omega,\ X=(R,\theta)$$
$$\frac{\partial\psi(X)}{\partial n} = 10\cos 2\theta \qquad X \in \partial\Omega,$$

which does not have any known exact solution.

Table 3 shows certain numerical values of the solution. Graphical representation is given in Fig. 7.

Table 3

$N = 10,\ X_i\ [\frac{1}{3},\theta_i],\ \upsilon=0.01$

I	θ_i	Numerical solution
1	0.0000	−0.5916
2	0.5236	5.6260
3	1.0472	6.2457
4	1.5708	0.6002
5	2.0944	−5.6564
6	2.6180	−2287
7	3.1416	−0.5915
8	3.6652	5.6260
9	4.1888	6.2457
10	4.7124	0.6002
11	5.2360	−5.6564
12	5.7596	−6.2287

FIG.7 THE NUMERICAL SOLUTION

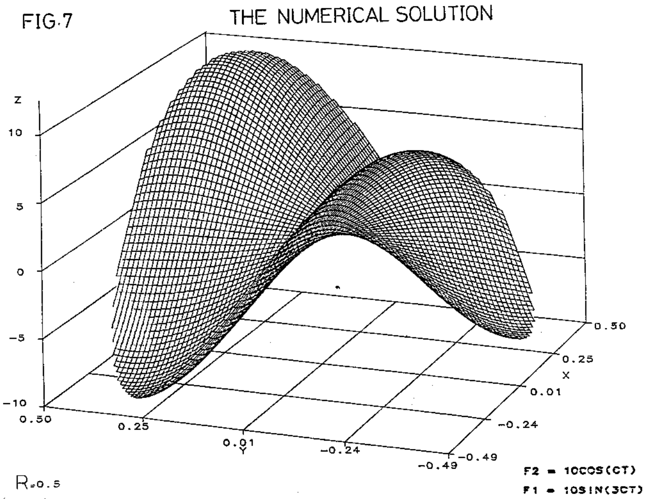

Example 3

We solve

$$\Delta^2\psi(X) = 0, \qquad X \in \Omega,$$
$$\psi(X) = 10\sin\theta \qquad X \in \partial\Omega,\ X = (R,\theta)$$
$$\frac{\partial\psi(X)}{\partial n} = 10\cos 3\theta$$

Table 4 gives certain numerical values of the solution.

Table 4

$N = 10,\ X_i = [\frac{1}{3},\theta_i],\ \upsilon = 0.01$

I	θ_i	Numerical solution
1	0.0000	−0.1535
2	0.3927	3.11916
3	0.7854	2.4284
4	1.1781	−1.4241
5	1.5708	−3.6167
6	1.9635	−1.3065
7	2.3562	2.6455
8	2.7489	3.4754
9	3.1416	0.1535
10	3.5343	−3.1916
11	3.9270	−2.4284
12	4.3197	1.4241
13	4.7124	3.6167
14	5.1051	1.3065
15	5.4978	−2.6455
16	5.8905	−3.4754

A graphical representation is shown in Fig. 8. One can clearly see the periodicity of ψ in the figure.

FIG.8 NUMERICAL SOLUTION

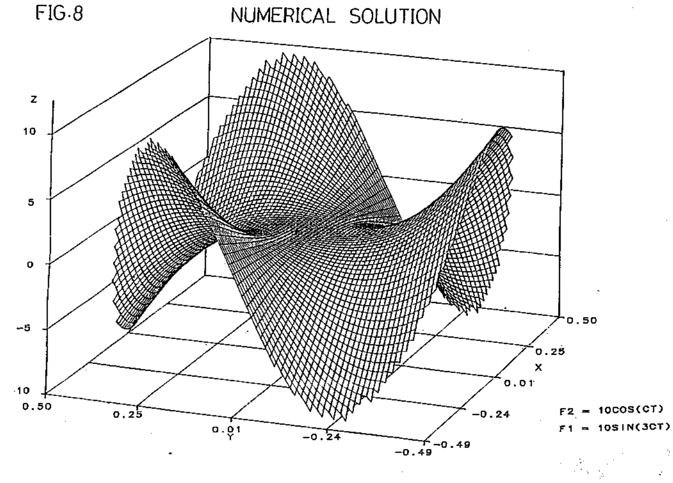

REFERENCES

Brebbia C.A. (Editor), 1981. Boundary element methods, Proceeding of the third international Seminar, Irvine, California, July 1981, CML Publications, Springer - Verlag, Berlin, Heidelberg, New York.

Brebbia C.A. and **W.S. Venturini, (Editors), 1987.** Boundary element techniques, Applications in stress analysis and heat transfer. Computational Mechanics Publications.